Ground-state behavior of the 3d $\pm J$ random-bond Ising model

Alexander K. Hartmann
hartmann@tphys.uni-heidelberg.de
Institut für theoretische Physik, Philosophenweg 19,
69120 Heidelberg, Germany
Tel. +49-6221-549449, Fax. +49-6221-549331
(December 1, 1998)

Large numbers of ground states of the three-dimensional $\pm J$ random-bond Ising model are calculated for sizes up to 14^3 using a combination of a genetic algorithm and Cluster-Exact Approximation. Several quantities are calculated as function of the concentration p of the antiferromagnetic bonds. The critical concentration where the ferromagnetic order disappears is determined using the Binder cumulant of the magnetization. A value of $p_c = 0.222 \pm 0.005$ is obtained. From the finite-size behavior of the Binder cumulant and the magnetization critical exponents $\nu = 1.1 \pm 0.3$ and $\beta = 0.2 \pm 0.1$ are calculated.

The behavior of the distribution of overlaps $P(q)$ is used to investigate how the spin-glass phase evolves with increasing concentration p. The spin-glass order is characterized by a broad distribution of overlaps which extends down to $q = 0$.

Keywords (PACS-codes): Spin glasses and other random models (75.10.Nr), Numerical simulation studies (75.40.Mg), General mathematical systems (02.10.Jf).

INTRODUCTION

In this work systems of N spins $\sigma_i = \pm 1$, described by the Hamiltonian

$$H \equiv - \sum_{\langle i,j \rangle} J_{ij} \sigma_i \sigma_j \qquad (1)$$

are investigated. The spins are placed on a three-dimensional (d=3) cubic lattice of linear size L with periodic boundary conditions in all directions. Systems with quenched disorder of the nearest-neighbor interactions (bonds) are investigated. Their possible values are $J_{ij} = \pm 1$. The concentration of the antiferromagnetic (AF) bonds ($J_{ij} = -1$) is denoted with p, all other $(1-p)$ interactions are ferromagnetic. A constrained is imposed, so that the fraction of the antiferromagnetic bonds is exactly p for all realizations of the disorder.

The model shows a complex behavior for low temperatures. For large concentrations of the ferromagnetic bonds it is energetically favorable for two interacting spins to have the same orientation. Hence, the system shows ferromagnetic order, which means that most of the spins have the same value. For large concentrations p the system is antiferromagnetically ordered: the system can be divided into to penetrating sublattices and each sublattice has ferromagnetic order, but the sign of the ordering of the two sublattices is different. For intermediate concentrations of the antiferromagnetic bonds neither ferromagnetic nor antiferromagnetic order exists. The system is called a spin glass [1]. For finite-dimensional spin glasses no final agreement about their behavior exists. Recent results from simulations [2,3] of small systems with $p = 0.5$ up to size 16^3 indicate that the three-dimensional spin glass has a complex behavior: the (free) energy landscape has many stable configurations which differ strongly from each other. Whether the onset of this spin-glass behavior takes place at the same concentration where the ferromagnetic order disappears is unclear.

Here the ground-state, i.e. zero temperature ($T = 0$), behavior of the model as function of the concentration p is investigated. Since the phase diagram of the system is symmetrical to $p = 0.5$ if one identifies the ferromagnetic with the antiferromagnetic regime, only values $p < 0.5$ are used. Of special interest is the critical concentration p_c where the ferromagnetic order disappears.

In the past the $\pm J$ random-bond Ising model has been studied using Monte-Carlo simulations [4], zero-temperature series expansions [5], high-temperature series expansions [6–8], Monte Carlo renormalization-group calculations [9] and renormalization-group theory [10]. All of these results are qualitatively consistent with the phase-diagram described above, but no agreement is found on the value of the critical concentration p_c or its temperature dependence. In all of these publications the detailed distribution of the states was not investigated, which can be done for example by calculating the distribution of overlaps.

A study of this model using true ground states has not been performed before. Only for special two-dimensional systems, where exact ground states can be calculated efficiently, some results [11–13] are known. There the critical concentration of a square lattice is estimated to be $p_c^{2d} = 0.10$.

The behavior of the $\pm J$ random bond Ising model is determined by the occurrence of *frustration* [14]. The simplest example of a frustrated system is a triple of spins where all pairs are connected by antiferromagnetic bonds. It is not possible to find a spin-configuration were all bonds contribute with a negative value to the energy. One says that it is not possible to *satisfy* all bonds. In general a system is frustrated, if closed loops of bonds exists, where the product of these bond-values is negative. For square and cubic systems the smallest closed loops consist of four bonds. They are called (elementary) *plaquettes*.

The presence of frustration makes the calculation of exact ground states of such systems computationally hard. Only for the special case of the two-dimensional system with periodic boundary conditions in no more than one direction and without external field a polynomial-time algorithm is known [15].

For the general case the simplest method works by enumerating all 2^N possible states and has obviously an exponential time complexity. Even a system size of 4^3 is too large. The basic idea of the *Branch-and-Bound* algorithm [16] is to exclude parts of the state-space, where no low-lying states can be found. Using this method the complete low-energy landscape of systems of size 4^3 can be calculated [17].

A more sophisticated method called *Branch-and-Cut* [18,19] works by rewriting the energy as a linear function and an additional set of inequalities which must hold for the solution. Since not all inequalities are known a priori the method iteratively solves the linear problem, looks for inequalities which are violated, and adds them to the set until the solution is found. Since the number of inequalities grows exponentially with the system size the same holds for the computation time of the algorithm. With Branch-and-Cut anyway small systems up to 8^3 are feasible. The method used here is able to calculate true ground states up to size 14^3.

By studying ground states one does not encounter ergodicity problems or critical slowing down like in Monte-Carlo simulations. Since it is possible to compare with exact results from Branch-and-Cut calculations no uncontrolled approximations are used. The only uncertainty comes from the fact that one is restricted to relatively small systems.

In the next section a short description of the method is presented. Afterwards the results are presented. In the last section a conclusion is driven.

ALGORITHM

The algorithm for the calculation of the ground states bases on a special genetic algorithm [20,21] and on *Cluster-Exact Approximation* (CEA) [22] which is an optimization method designed especially for spin glasses. Next a short sketch of these algorithms is given.

Genetic algorithms are biologically motivated. An optimal solution is found by treating many instances of the problem in parallel, keeping only better instances and replacing bad ones by new ones (survival of the fittest). The genetic algorithm starts with an initial population of M_i randomly initialized spin configurations (= *individuals*), which are linearly arranged in a ring. Then $n_o \times M_i$ times two neighbors from the population are taken (called *parents*) and two offsprings are created using a triadic crossover: a mask is used which is a third randomly chosen (usually distant) member of the population with a fraction of 0.1 of its spins reversed. In a first step the offsprings are created as copies of the parents. Then those spins are selected, where the orientations of the first parent and the mask agree [23]. The values of these spins are swapped between the two offsprings. Then a *mutation* with a rate of p_m is applied to each offspring, i.e. a fraction p_m of the spins is reversed.

Next for both offsprings the energy is reduced by applying CEA: The method constructs iteratively and randomly a non-frustrated cluster of spins. Spins adjacent to many unsatisfied bonds are more likely to be added to the cluster. During the construction of the cluster a local gauge-transformation of the spin variables is applied so that all interactions between cluster spins become ferromagnetic.

Fig. 1 shows an example of how the construction of the cluster works using a small spin-glass system. For 3d $\pm J$ spin glasses each cluster contains typically 58 percent of all spins. The non-cluster spins act like local magnetic fields on the cluster spins, therefore the ground state of the cluster is not trivial. Since the cluster has only ferromagnetic interactions, an energetic minimum state for its spins can be calculated in polynomial time by using graph theoretical methods [24–26]: an equivalent network is constructed [27], the maximum flow is calculated [28,29] and the spins of the cluster are set to their orientations leading to a minimum in energy. This minimization step is performed $n_{\min}$ times for each offspring.

Afterwards each offspring is compared with one of its parents. The pairs are chosen in the way that the sum of the phenotypic differences between them is minimal. The phenotypic difference is defined here as the number of spins where the two configurations differ. Each parent is replaced if its energy is not lower (i.e. not better) than the corresponding offspring. After this whole step is done $n_o \times M_i$ times, the population is halved: From each pair of neighbors the configuration which has the higher energy is eliminated. If more than 4 individuals remain the process is continued otherwise it is stopped and the best individual is taken as result of the calculation.

The whole algorithm is performed n_R times and all configurations which exhibit the lowest energy are stored, resulting in n_G statistically independent ground-state configurations.

This algorithm was already applied to examine the ground-state landscape of 3d spin glasses [3].

RESULTS

We used the simulation parameters determined in former calculations for $p = 0.5$: For each system size many different combinations of the simulation parameters m_i, n_o, n_{min}, p_m were tested. For the final parameter sets it is not possible to obtain lower energies even by using parameters where the calculation consumes four times the computational effort. Here a mutation rate of $p_m = 0.2$ and $n_R = 10$ runs per realisation were used for all system sizes.

For smaller concentrations p the ground states are easier to find, because the number of frustrated plaquettes is smaller. But it was not possible to reduce the computational effort substantially in order to get still ground states. Consequently, we used the parameters of $p = 0.5$ for all concentrations p. Table 1 summarizes the parameters. Also the typical computer time τ spent per run on a 80 MHz PPC601 is given. Using these parameters on average $n_G > 8$ ground states were obtained for every system size L using $n_R = 10$ runs per realization.

We compared our results for 180 sample systems of $L = 6$ with exact ground states which were obtained using a Branch-and-Cut program [18,19]. The genetic CEA algorithm found the true ground states for all systems! The same result was obtained for $L = 4$ as well. For $L > 6$ the Branch-and-Cut program needs to much computer time because of the exponential running time. A more detailed analysis is presented in [30]. Hence, we can be sure that genetic CEA and our method of choosing the parameters lead to true ground states or at least to states very close to true ground states.

We performed ground state calculations for $p \in [0.1, 0.4]$ for lattice sizes $L = 3, 4, 5, 6, 8, 10, 14$. For the largest size $N_L = 1000$ independent realizations were taken. For smaller systems this number could be raised up to 30000. Most of the systems have AF-bond concentrations around $p = 0.22$

The ground state energy e as function of system size for different system sizes is shown in Fig 2. To keep the figure clear only the sizes $L = 3, 4, 6, 14$ are presented. For small concentrations p the ground state is mainly ferromagnetic. It follows that all AF bonds are not satisfied, thus the ground state energy increases linearly like $e(p) \approx -3 + 6p$ with p. For larger concentrations the ground state energy approaches the $p = 0.5$ limit, because the spins can arrange so that not all AF-bonds are broken. With increasing L the ground state energy decreases, because the periodic boundary conditions impose less constraints on the system. For $L \to \infty$ and $p = 0.5$ a ground state energy of $e_\infty(0.5) = -1.7876(3)$ is found in [3].

From fig. 2 is clear that the energy as function of concentration is not well suited for determining the critical concentration p_c where the ferromagnetic behavior disappears. For this purpose the Binder cumulant [31,32]

$$g(p, L) \equiv \frac{1}{2}\left(3 - \frac{\langle M^4\rangle}{\langle M^2\rangle^2}\right) \qquad (2)$$

for the magnetization $M \equiv \frac{1}{N}\sum_i \sigma_i$ is evaluated. The average $\langle \ldots \rangle$ denotes both average over different ground states of a realization and over the disorder. In fig. 3 the Binder cumulant is shown for $L = 3, 5, 8, 10, 14$. $L = 4, 6$ are omitted in this figure to keep it clear. For the same reason only typical error bars for two sample points are shown. All curves intersect at $p_c = 0.222 \pm 0.002$. Only $L = 4$ (not shown) is little worse, because it meets the others in the interval $p \in [0.217, 0.222]$. We conclude that the critical concentration for the ferromagnetic order is $p_c = 0.222(5)$.

The value for p_c is comparable to results from high-temperature series expansions: $p_c = 0.19(2)$ [6], $p_c \approx 0.25$ [7], $p_c = 234(2)$ [33] from Monte-Carlo renormalization-group results $p_c = 0.233(4)$ [9] and from Monte-Carlo simulations: $p_c \approx 0.24$ [4]. Our value is much larger than a result from a zero-temperature expansion: $p_c = 0.12-0.13$ [5] and much lower than a recent result from a renormalization-group study: $p_c \approx 0.37$ [10]. Since the intersection of the curves of the Binder cumulant is very sharp, we believe that our result is very reliable, although the systems investigated here are rather small.

For the Binder cumulant the following finite-size scaling relation is assumed [32]

$$g(p, L) = \tilde{g}(L^{1/\nu}(p - p_c)) \qquad (3)$$

By plotting $g(p, L)$ against $L^{1/\nu}(p-p_c)$ with correct parameter ν the datapoints for different system sizes should collapse onto a single curve. The best results were obtained for $p_c = 0.222$ and $1/\nu = 0.9$. In fig. 4 the resulting scaling plot is shown. It is possible to change the value of ν in a wide range without large effects on the scaling plot. We estimate $\nu = 1.1(3)$. This is consistent with $\nu = 1.7(3)$ which was found using Monte-Carlo simulations of spin glasses ($p = 0.5$) at finite temperature [34].

The average magnetization $m \equiv \langle M \rangle$ has the standard finite-size scaling form [35]

$$m(p, L) = L^{-\beta/\nu}\tilde{m}(L^{1/\nu}(p - p_c)) \qquad (4)$$

By plotting $L^{\beta/\nu}m(p, L)$ against $L^{1/\nu}(p-p_c)$ with correct parameters β, ν the datapoints for different system sizes should collapse onto a single curve. The best result was obtained using $1/\nu = 0.9$ and $\beta/\nu = 0.19$. It is shown in fig. 5 for $L = 3, 5, 8, 10, 14$. From variations of the value β/ν we estimate the value of the exponent $\beta = 0.2(1)$.

So far the behavior of the ferromagnetic regime and related characteristic values were investigated. As explained before the model shows a spin-glass phase for intermediate concentrations of the antiferromagnet bonds. To characterize this spin-glass behavior now the overlap q is used. It compares two different states $\{\sigma_i^\alpha\}, \{\sigma_i^\beta\}$ of the same realization of the random bonds

$$q^{\alpha\beta} \equiv \frac{1}{N}\sum_i \sigma_i^\alpha \sigma_i^\beta \qquad (5)$$

For ferromagnetic/antiferromagnetic order two independently calculated ground states are identical or related by a global flip of all spins, i.e. $q = \pm 1$. For spin-glass order many different ground states exist [3], consequently q can take also intermediate values $q \in [-1, 1]$.

Since the system has no external field, each state is equivalent to the state where all spins are reversed, consequently only the absolute value $|q|$ is considered here.

In fig. 6 the average value of the overlap $\langle |q| \rangle \equiv \langle |q^{\alpha\beta}| \rangle$ is shown for the lattice sizes $L = 3, 4, 8, 14$. The decrease of $\langle |q| \rangle$ with increasing concentration p is clearly visible. Since this quantity has much larger fluctuations than the magnetization, it is difficult to use this data for further analysis. Also the value stays below 1.0 for a large interval, hence it is not possible to extract at which concentration the onset of the spin-glass behavior is located.

More information about the spin-glass phase can be obtained, if one calculates not only the average of $|q|$, but its distribution [36]

$$P(|q|) \equiv \langle \delta(|q| - |q^{\alpha\beta}|) \rangle \tag{6}$$

which can be used to describe the ground-state landscape. In fig. 7 the distributions for sizes $L = 3, 4, 8, 14$ at $p \approx 0.18$ are presented[1]. With increasing size the distributions becomes narrower. The reason is, that due to the discrete bond distribution $J_{ij} = \pm 1$ there are always some small clusters of spins, which can take two orientations in the ground state. With increasing system size L these effects cancel out and $P(|q|)$ converges to a delta-function $\delta(q - q_{free})$, where q_{free} is just the fraction of spins not contained in such free clusters. This ground-state landscape is similar to that of random-field Ising systems [37].

In fig. 8 the distributions of overlaps is displayed for a concentration slightly larger than p_c. Here the behavior is completely different. The distributions extend over a large interval down to $q = 0$. With increasing lattice size L only the shape of the large-q part changes a little bit while for small values no systematic modification is visible. The peak at large q-values, which raises with increasing concentration p, results from small clusters of spins which can take two orientations in the ground state. This is the same as for smaller concentrations of the AF-bonds. But the large extent down to $q = 0$ cannot be explained in this way. It shows that spin-glass ground states have a very rich ordering, similar to the behavior found for the SK-model [36], where each spin interacts with every other spin (for a detailed discussion of the ground-state landscape see [3,38]).

To investigate this behavior quantitatively the variance $\sigma^2(|q|)$ of the distributions as function of AF-bond concentration p and system size L is calculated

$$\sigma^2(|q|) \equiv \langle (|q^{\alpha\beta}| - \langle |q| \rangle)^2 \rangle \tag{7}$$

[1] Since all realizations of a given size L have exactly the same number of ferromagnetic bonds, for each system size only a finite number of different concentrations is possible. Here for each lattice size the value of p is chosen which is nearest to 0.18

In fig. 9 the result for $L = 3, 4, 8, 14$ is shown. For small concentration p the width of the distributions is small and shrinks with increasing size L. For larger concentrations the width increases and remains nonzero even for larger lattice sizes. In [3] it was shown, that the spin glass ground state with $p = 0.5$ is likely to have a broad distribution even for $L \to \infty$. For larger sizes the statistics is too bad to extract for example a critical concentration $p_c^{(2)}$ by a finite-size scaling analysis similar to that presented above.

The onset of the spin glass behavior can even better be observed by calculating the fraction X_{q_0} of the distribution of overlaps below a fixed value q_0:

$$X_{q_0} \equiv \int_0^{q_0} P(|q|)\, dq \tag{8}$$

In fig. 10 the value of $X_{0.5}$ is shown as function of p for the lattice sizes $L = 3, 4, 8, 14$. For the limiting case $p = 0.5$ the value of $X_{0.5}$ converges to a nonzero value for $L \to \infty$ [39].

CONCLUSION

Using a combination of a genetic algorithm and Cluster-Exact Approximation ground states of the three-dimensional $\pm J$ random-bond Ising model were calculated for different concentrations of the antiferromagnetic bonds. A former comparison with exact ground states calculated using a Branch-and Cut program shows that genetic CEA is able to calculate true ground states.

For small concentrations the ground state is mainly ferromagnetic. The critical concentration where the ferromagnetic order disappears was determined using the Binder-cumulant $g(p, L)$ of the magnetization:

$$p_c = 0.222 \pm 0.005 \tag{9}$$

This is the first time p_c is calculated by direct investigations of ground states.

Using a finite-size scaling analysis of the magnetization and the Binder-cumulant critical exponents were obtained:

$$\nu = 1.1 \pm 0.3,\ \beta = 0.2 \pm 0.1 \tag{10}$$

These values are consistent with results from Monte-Carlo simulations of the $p = 0.5$ case at finite temperature, where the same analysis presented here was performed for the spin-glass order parameter q instead of the magnetization m.

The onset of the spin-glass behavior with increasing lattice size was investigated the first time by calculating the distributions of overlaps as function of p. The spin glass phase is characterized by a broad distribution of overlaps which extends down to $q = 0$ and does not change substantially with increasing system size. For this quantity the bad statistics for larger values of the concentration $p > 0.23$ does not allow to determine a second critical concentration $p_c^{(2)}$. Hence, it is yet not possible to check whether the ferromagnetic order disappears at the same concentration where the spin-glass phase appears. Here much more data is needed.

ACKNOWLEDGEMENTS

The author thanks H. Horner and G. Reinelt for manifold support. He is grateful to M. Jünger, M. Diehl and T. Christof who put a Branch-and-Cut program for the exact calculation of spin-glass ground states of small systems at his disposal. He thanks R. Kühn for critical reading of the manuscript and for giving many helpful hints. This work was engendered by interesting discussions with J. Bendisch at the "Algorithmic Techniques in Physics" seminar held at the *International Conference and Research Center for Computer Science Schloss Dagstuhl* in Wadern/Germany. The author took much benefit from discussions with S. Kobe, H. Rieger and A.P. Young. He thanks F. Hucht for supplying the program *fsscale* for performing the finite-size scaling analysis. He is also grateful to the *Paderborn Center for Parallel Computing* for the allocation of computer time. This work was supported by the Graduiertenkolleg "Modellierung und Wissenschaftliches Rechnen in Mathematik und Naturwissenschaften" at the *Interdisziplinäres Zentrum für Wissenschaftliches Rechnen* in Heidelberg.

---

[1] For reviews on spin glasses see: K. Binder and A.P. Young, Rev. Mod. Phys. **58**, 801 (1986); K.H. Fisher and J.A. Hertz, Spin Glasses, Cambridge University Press, 1991
[2] E. Marinari, G. Parisi, J.J. Ruiz-Lorenzo und F. Ritort, Phys. Rev. Lett. **76**, 843 (1996)
[3] A.K. Hartmann, Europhys. Lett. **40**, 429 (1997)
[4] S. Kirkpatrick, Phys. Rev. B **16**, 4630 (1977)
[5] G. Grinstein, C. Jayaprakash and M. Wortis, Phys. Rev. B **19**, 260 (1979)
[6] J.D. Reger and A. Zippelius, Phys. Rev. Lett. **57**, 3225 (1986)
[7] R. Fisch, Phys. Rev. B **44**, 652 (1991)
[8] R.R.P. Singh, Phys. Rev. Lett **67**, 899 (1991)
[9] Y. Ozeki and H. Nsihimori, J. Phys. Soc. Jpn. **56** 1568 (1987); J. Phys. Soc. Jpn. **56** 2992 (1987)
[10] G. Migliorini and A. N. Berker, Phys. Rev. B **57**, 426 (1998)
[11] J. Bendisch, J. Stat. Phys. **67**, 1209 (1992)
[12] J. Bendisch, Physica A **202**, 48 (1994)
[13] N. Kawashima and H. Rieger, Europhys. Lett. **39**, 85 (1997)
[14] G. Toulouse, Commun. Phys. **2**, 115 (1977)
[15] F. Barahona, R. Maynard, R. Rammal and J.P. Uhry, J. Phys. A **15**, 673 (1982).
[16] A. Hartwig, F. Daske and S. Kobe, Comp. Phys. Commun. **32** 133 (1984)
[17] T. Klotz and S. Kobe, J. Phys. A: Math. Gen. **27**, L95 (1994)
[18] C. De Simone, M. Diehl, M. Jünger, P. Mutzel, G. Reinelt and G. Rinaldi, J. Stat. Phys. **80**, 487 (1995)
[19] C. De Simone, M. Diehl, M. Jünger, P. Mutzel, G. Reinelt and G. Rinaldi, J. Stat. Phys. **84**, 1363 (1996)
[20] K.F. Pál, Physica A **223**, 283 (1996)
[21] Z. Michalewicz, Genetic Algorithms + Data Structures = Evolution Programs, Springer, Berlin 1992
[22] A.K. Hartmann, Physica A, **224**, 480 (1996)
[23] K.F. Pál, Biol. Cybern. **73**, 335 (1995)
[24] J.D. Claiborne, Mathematical Preliminaries for Computer Networking, Wiley, New York 1990
[25] W. Knödel, Graphentheoretische Methoden und ihre Anwendung Springer, Berlin 1969
[26] M.N.S. Swamy and K. Thulasiraman, Graphs, Networks and Algorithms (Wiley, New York 1991)
[27] J.-C. Picard and H.D. Ratliff, Networks **5**, 357 (1975)
[28] J.L. Träff, Eur. J. Oper. Res. **89**, 564 (1996)
[29] R.E. Tarjan, Data Structures and Network Algorithms, Society for industrial and applied mathematics, Philadelphia 1983
[30] A.K. Hartmann, to appear in Phys. Rev. E, preprint cond-mat/9806114
[31] K. Binder, Z. Phys. B **43**, 119 (1981)
[32] R.N. Bhatt and A.P. Young, Phys. Rev. Lett. **54**, 924 (1985); Phys. Rev. B **37**, 5606 (1988)
[33] R. Fisch, private communication, using [8]
[34] N. Kawashima and A.P. Young, Phys. Rev. B **53**, R484 (1996)
[35] K. Binder and D.W. Heermann, Monte Carlo Simulations in Statistical Physics, Springer 1988
[36] G. Parisi, Phys. Rev. Lett. 43, 1754 (1979); J. Phys. A 13, 1101 (1980); 13, 1887 (1980); 13, L115 (1980); Phys. Rev. Lett. 50, 1946 (1983).
[37] A.K. Hartmann, Physica A **248**, 1 (1998)
[38] A.K. Hartmann, Europhys. Lett. bf 44, 249 (1998)
[39] A.K. Hartmann, in preparation

Captions

Fig. 1 Example of the Cluster-Exact Approximation method. A part of a spin glass is shown. The circles represent lattice sites/spins. Straight lines represent ferromagnetic bonds the jagged lines antiferromagnetic interactions. The top part shows the initial situation. The construction starts with the spin at the center. The bottom part displays the final stage. The spins which belong to the cluster carry a plus or minus sign which indicates how each spin is transformed, that only ferromagnetic interactions remain inside the cluster. All other spins cannot be added to the cluster because it is not possible to multiply them by ± 1 to make all adjacent bonds positive. Please note that many other combinations of spins can be used to build a cluster without frustration.

Fig. 2 Average ground state energy e per spin as function of AF-bond concentration p for system sizes $L = 3, 4, 6, 14$. Lines are guides for the eyes only.

Fig. 3 Binder cumulant of magnetization as function of AF-bond concentration p for system size $L = 3, 5, 8, 10, 14$. Two typical error bars are given. Lines are guides for the eyes only.

Fig. 4 Scaled plot of Binder cumulant. Line is guide for the eyes only.

Fig. 5 Scaled plot of magnetization. The inset show the raw data for $L = 3, 5, 14$. Lines are guides for the eyes only.

Fig. 6 Average overlap $\langle |q| \rangle$ value as function of AF-bond concentration p for $L = 3, 4, 8, 14$. With increasing concentration more and more spins belong to clusters which contribute to the degeneracy of the ground state, thus the average overlap value decreases. Where the onset of the spin glass behavior is located exactly cannot be seen from this figure. Lines are guides for the eyes only.

Fig. 7 Distribution $P(|q|)$ of overlaps for AF-bond concentrations about $p \approx 0.18$ for $L = 3, 4, 8, 14$. A finite fraction of spins is contained in small clusters which can take two orientations in the ground state. For $L \to \infty$ a delta-function is obtained similar to the distribution found for the ground states of random-field Ising systems. Lines are guides for the eyes only.

Fig. 8 Distribution $P(|q|)$ of overlaps for AF-bond concentrations about $p \approx 0.23$ for $L = 3, 4, 8, 14$. The distribution is broad and extends to $q = 0$ for all sizes L, indicating a spin-glass behavior. Lines are guides for the eyes only.

Fig. 9 Average variance $\sigma^2(|q|)$ of overlap distribution as function of AF-bond concentration p. For small concentrations the width of the distribution shrinks to zero with increasing size L. For larger values the spin-glass phase is characterized by broad distributions of overlaps. Lines are guides for the eyes only.

Fig. 10 Average fraction $X_{0.5}$ of overlap distribution below $q = 0.5$ as function of AF-bond concentration p for sizes $L = 3, 4, 8, 14$. In the spin-glass phase the distribution of overlaps extends to $q = 0$ for all lattice sizes. Lines are guides for the eyes only.

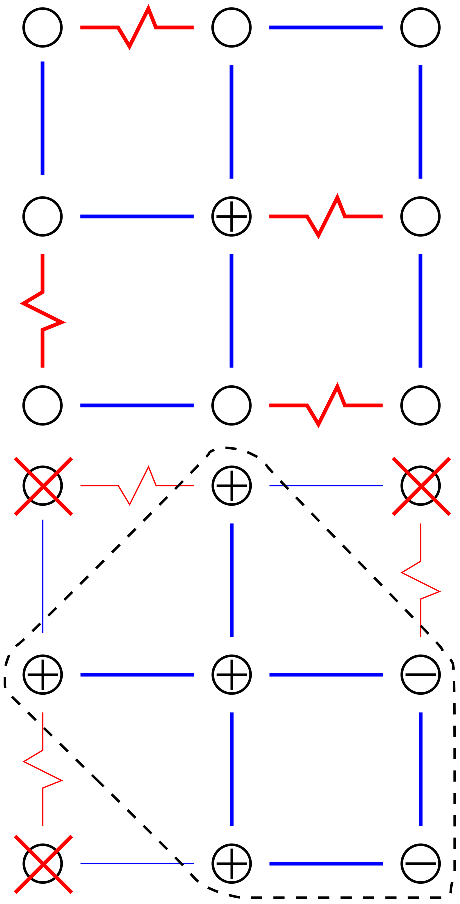

FIG. 1. Example of the Cluster-Exact Approximation method. A part of a spin glass is shown. The circles represent lattice sites/spins. Straight lines represent ferromagnetic bonds the jagged lines antiferromagnetic interactions. The top part shows the initial situation. The construction starts with the spin at the center. The bottom part displays the final stage. The spins which belong to the cluster carry a plus or minus sign which indicates how each spin is transformed, that only ferromagnetic interactions remain inside the cluster. All other spins cannot be added to the cluster because it is not possible to multiply them by ± 1 to make all adjacent bonds positive. Please note that many other combinations of spins can be used to build a cluster without frustration.

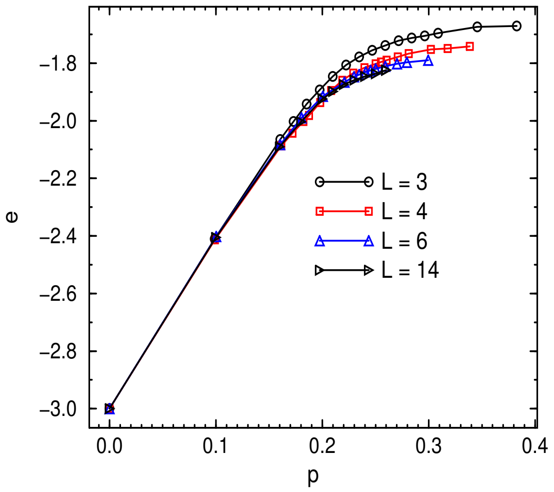

FIG. 2. Average ground state energy e per spin as function of AF-bond concentration p for system sizes $L = 3, 4, 6, 14$. Lines are guides for the eyes only.

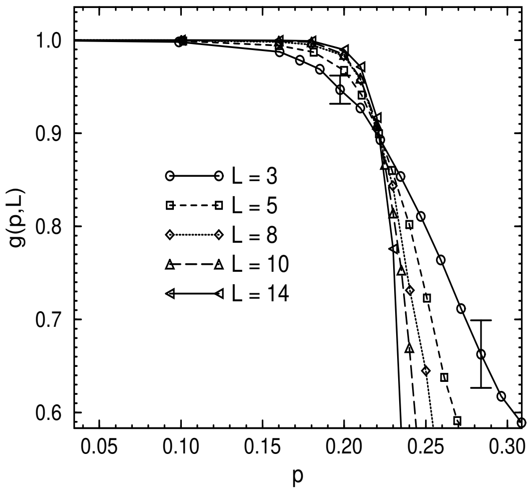

FIG. 3. Binder cumulant of magnetization as function of AF-bond concentration p for system size $L = 3, 5, 8, 10, 14$. Two typical error bars are given. Lines are guides for the eyes only.

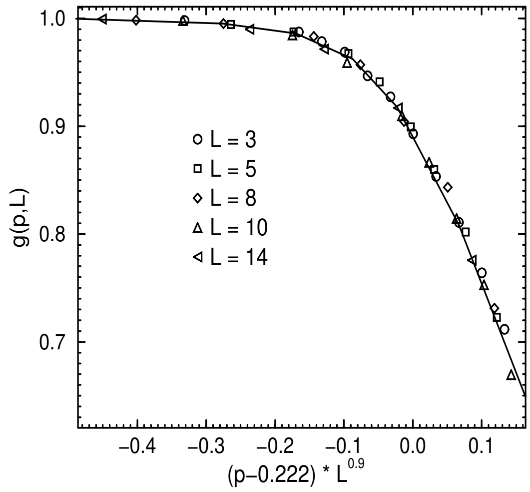

FIG. 4. Scaled plot of Binder cumulant. Line is guide for the eyes only.

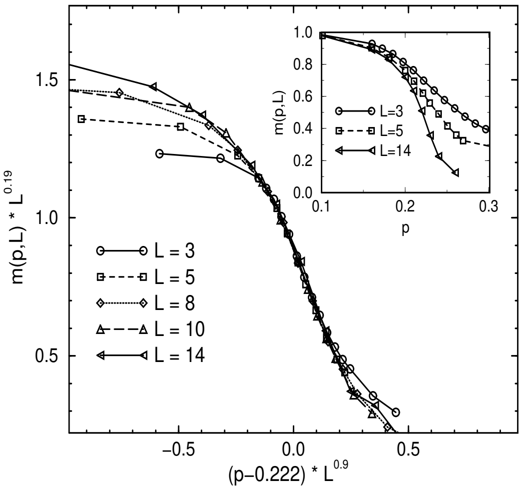

FIG. 5. Scaled plot of magnetization. The inset show the raw data for $L = 3, 5, 14$. Lines are guides for the eyes only.

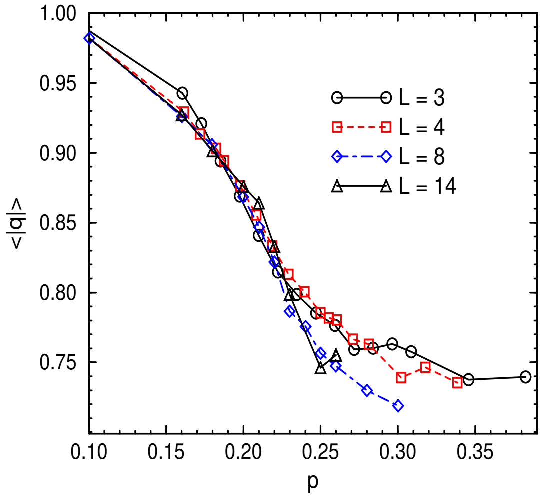

FIG. 6. Average overlap $\langle |q| \rangle$ value as function of AF-bond concentration p for $L = 3, 4, 8, 14$. With increasing concentration more and more spins belong to clusters which contribute to the degeneracy of the ground state, thus the average overlap value decreases. Where the onset of the spin glass behavior is located exactly cannot be seen from this figure. Lines are guides for the eyes only.

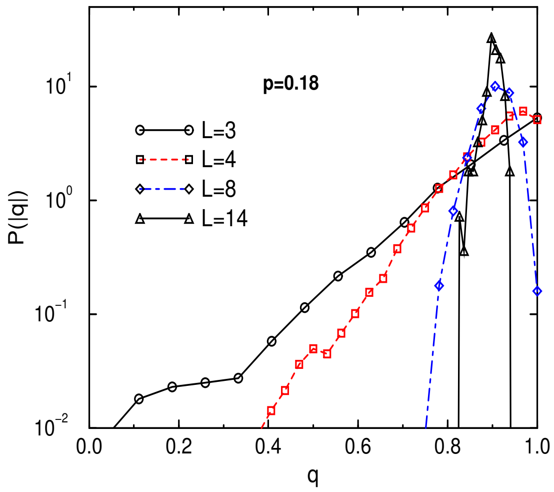

FIG. 7. Distribution $P(|q|)$ of overlaps for AF-bond concentrations about $p \approx 0.18$ for $L = 3, 4, 8, 14$. A finite fraction of spins is contained in small clusters which can take two orientations in the ground state. For $L \to \infty$ a delta-function is obtained similar to the distribution found for the ground states of random-field Ising systems. Lines are guides for the eyes only.

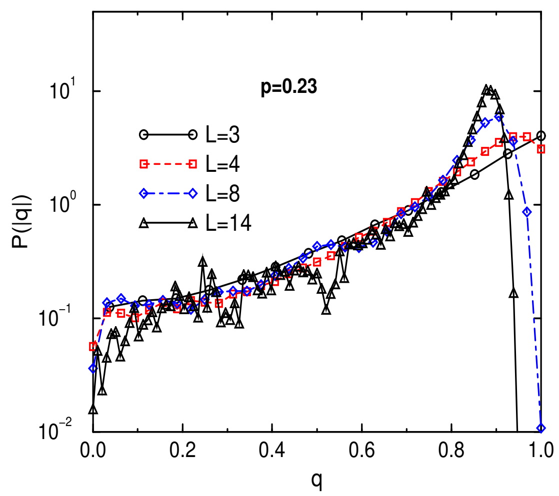

FIG. 8. Distribution $P(|q|)$ of overlaps for AF-bond concentrations about $p \approx 0.23$ for $L = 3, 4, 8, 14$. The distribution is broad and extends to $q = 0$ for all sizes L, indicating a spin-glass behavior. Lines are guides for the eyes only.

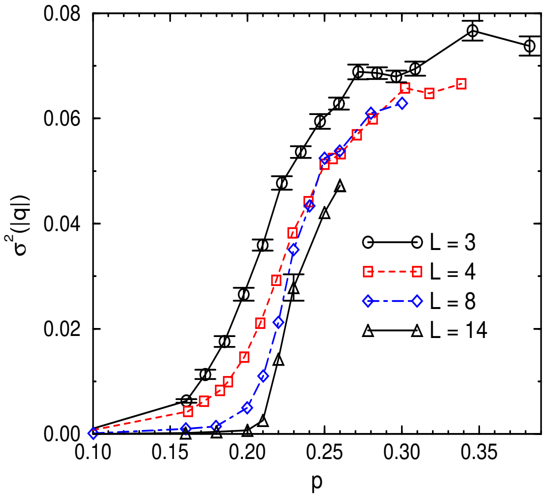

FIG. 9. Average variance $\sigma^2(|q|)$ of overlap distribution as function of AF-bond concentration p. For small concentrations the width of the distribution shrinks to zero with increasing size L. For larger values the spin-glass phase is characterized by broad distributions of overlaps. Lines are guides for the eyes only.

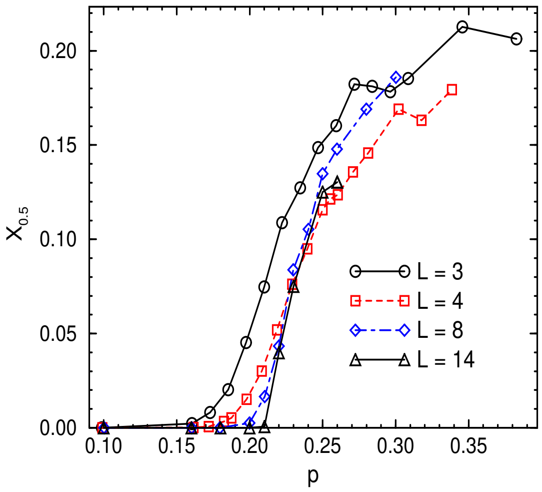

FIG. 10. Average fraction $X_{0.5}$ of overlap distribution below $q = 0.5$ as function of AF-bond concentration p for sizes $L = 3, 4, 8, 14$. In the spin-glass phase the distribution of overlaps extends to $q = 0$ for all lattice sizes. Lines are guides for the eyes only.

L	M_i	n_o	$n_{\min}$	τ (sec)
3	16	3	1	0.2
4	16	3	1	0.5
5	16	4	2	3
6	16	4	2	5
8	32	4	5	70
10	64	6	10	960
14	256	14	10	32400

Tab 1. Simulation parameters: L = system size, M_i = initial size of population, n_o = average number of offsprings per configuration, $n_{\min}$ = number of CEA minimization steps per offspring, τ = average computer time per ground state on a 80MHz PPC601.